Provided for non-commercial research and educational use only.
Not for reproduction, distribution or commercial use.

This chapter was originally published in the book *Methods in Enzymology,* Vol. 528 published by Elsevier, and the attached copy is provided by Elsevier for the author's benefit and for the benefit of the author's institution, for non-commercial research and educational use including without limitation use in instruction at your institution, sending it to specific colleagues who know you, and providing a copy to your institution's administrator.

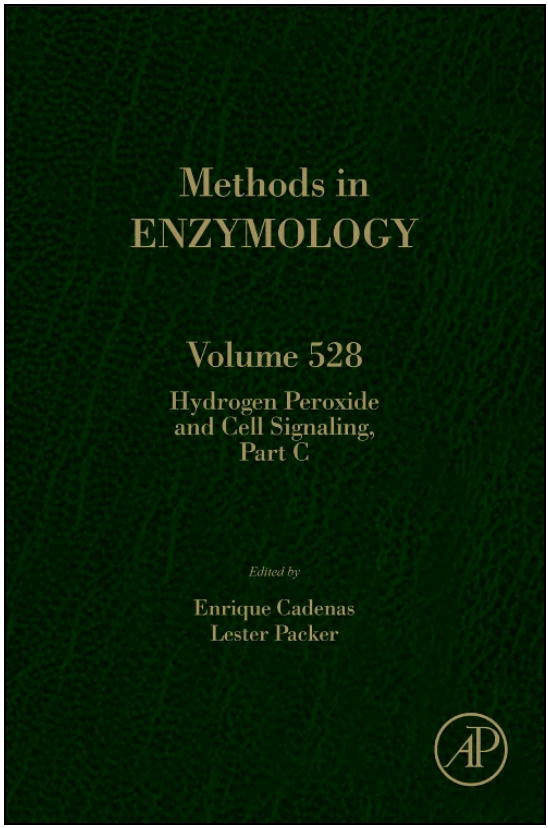

All other uses, reproduction and distribution, including without limitation commercial reprints, selling or licensing copies or access, or posting on open internet sites, your personal or institution's website or repository, are prohibited. For exceptions, permission may be sought for such use through Elsevier's permissions site at:
http://www.elsevier.com/locate/permissionusematerial

From Zachary D. Parsons, Kent S. Gates, Redox Regulation of Protein Tyrosine Phosphatases: Methods for Kinetic Analysis of Covalent Enzyme Inactivation.
In Enrique Cadenas And Lester Packer, editors: *Methods in Enzymology,* Vol. 528,
Burlington: Academic Press, 2013, pp. 129-154.
ISBN: 978-0-12-405881-1
© Copyright 2013 Elsevier Inc.
Academic Press

Author's personal copy

CHAPTER EIGHT

Redox Regulation of Protein Tyrosine Phosphatases: Methods for Kinetic Analysis of Covalent Enzyme Inactivation

Zachary D. Parsons*, Kent S. Gates*,†,1
*Department of Chemistry, University of Missouri, Columbia, Missouri, USA
†Department of Biochemistry, University of Missouri, Columbia, Missouri, USA
1Corresponding author: e-mail address: gatesk@missouri.edu

Contents

Abstract

Phosphorylation of tyrosine residues is an important posttranslational modification that modulates the function of proteins involved in many important cell signaling pathways. Protein tyrosine kinases and protein tyrosine phosphatases (PTPs) work in tandem to control the phosphorylation status of target proteins. Not surprisingly, the activity of some PTPs is regulated as part of the endogenous cellular mechanisms for controlling the intensity and duration of responses to various stimuli. One important mechanism for the regulation of PTPs involves endogenous production of hydrogen peroxide (H_2O_2) that inactivates enzymes via covalent modification of an active site cysteine

Methods in Enzymology, Volume 528
ISSN 0076-6879
http://dx.doi.org/10.1016/B978-0-12-405881-1.00008-2

© 2013 Elsevier Inc.
All rights reserved.

Author's personal copy

thiolate group. Other endogenous metabolites and xenobiotics that inactivate PTPs via covalent mechanisms also have the potential to modulate signal transduction pathways and may possess either therapeutic or toxic properties. This chapter discusses methods for quantitative kinetic analysis of covalent inactivation of PTPs by small molecules.

1. INTRODUCTION

Phosphorylation of tyrosine residues is an important posttranslational modification that modulates the function of proteins involved in many important cell signaling pathways (Hunter, 2000; Lemmon & Schlessinger, 2010; Tarrant & Cole, 2009; Tonks, 2006). The phosphorylation status of proteins that are regulated in this manner is controlled by the balanced action of protein tyrosine kinases (PTKs) that add a phosphoryl group to the hydroxyl group of a target tyrosine side chain and protein tyrosine phosphatases (PTPs) that catalyze hydrolytic removal of the phosphoryl group (Hunter, 2000; Lemmon & Schlessinger, 2010; Tarrant & Cole, 2009; Tonks, 2006). It has long been known that the cellular activity of PTKs is tightly regulated (Lemmon & Schlessinger, 2010) and there is growing recognition that the activity of PTPs can also be regulated as part of the cellular mechanisms for controlling the intensity and duration of response to a given stimulus (den Hertog, Groen, & van der Wijk, 2005; Östman, Frijhoff, Sandin, & Böhmer, 2011; Tonks, 2006). One important mechanism for the regulation of PTP activity involves generation of endogenous hydrogen peroxide (H_2O_2) by the highly controlled activation of NADPH oxidase (Nox) enzymes (Lambeth, 2004; Lambeth, Kawahara, & Diebold, 2007; Ushio-Fukai, 2006) in response to growth factors, hormones, and cytokines such as platelet-derived growth factor, epidermal growth factor, VEGF, insulin, tumor necrosis factor-α, and interleukin-1β (Dickinson & Chang, 2011; Rhee, 2006; Tonks, 2006; Truong & Carroll, 2012). Inactivation of purified PTPs *in vitro* by hydrogen peroxide proceeds via oxidation of the catalytic cysteine thiolate residue (Scheme 8.1; Denu & Tanner, 1998; Hecht & Zick, 1992; Heffetz, Bushkin, Dror, & Zick, 1990; Lee, Kwon, Kim, & Rhee, 1998; Tanner, Parson, Cummings, Zhou, & Gates, 2011). Despite the high sequence and structural homology of the catalytic subunits of classical PTPs (Barr et al., 2009), the oxidized forms of different family members have the potential to adopt significantly different structures, with the active site cysteine residue existing as either a sulfenic acid, disulfide, or sulfenyl amide (Scheme 8.1; Tanner et al., 2011). Reaction of the oxidized enzymes with

Author's personal copy

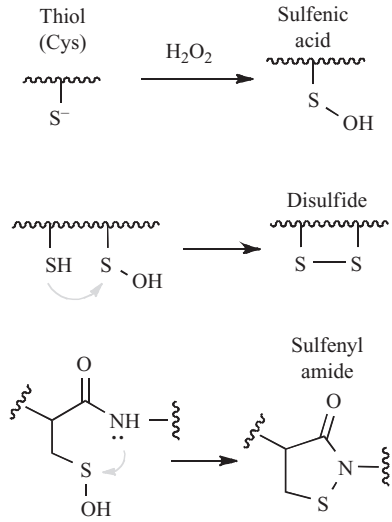

Scheme 8.1 Oxidative inactivation of PTPs.

low molecular weight or protein thiols leads to regeneration of the catalytically-active enzymes (Denu & Tanner, 1998; Parsons & Gates, 2013; Sivaramakrishnan, Cummings, & Gates, 2010; Sivaramakrishnan, Keerthi, & Gates, 2005; Tanner et al., 2011; Zhou et al., 2011).

The chemical and biochemical mechanisms underlying H_2O_2-dependent inactivation of PTPs in cells are not yet well understood. For example, the inactivation of intracellular PTPs during signaling events depends upon H_2O_2 and occurs rapidly (5–15 min; Lee et al., 1998; Mahedev, Zilbering, Zhu, & Goldstein, 2001; Meng, Buckley, Galic, Tiganis, & Tonks, 2004). However, the rate constants measured for inactivation of purified PTPs by H_2O_2 *in vitro* are modest (e.g., 10–40 M^{-1} s^{-1} for PTP1B; Denu & Tanner, 1998; Zhou et al., 2011). With rate constants in this range, the loss of PTP activity is anticipated to be rather sluggish at the low cellular concentrations of H_2O_2 expected to be present during signaling events ($t_{1/2}$ = 5–200 h at steady-state H_2O_2 levels of 0.1–1 μ*M*; Stone, 2006; Winterbourn, 2008). This kinetic discrepancy suggests that some unknown chemical or biochemical mechanism(s) in cells potentiates the ability of H_2O_2 to inactivate PTPs. Colocalization of PTP1B and Nox4 on the surface of the endoplasmic reticulum has been offered as a potential means for rapid and selective inactivation of this PTP during insulin signaling (Chen, Kirber, Yang, & Keaney, 2008). Others have provided evidence that localized inactivation of the peroxide-destroying enzyme,

Author's personal copy

peroxiredoxin, during cell signaling events may yield regions of high peroxide concentration that can drive rapid inactivation of PTPs in these locales (Woo et al., 2010). Alternatively, or in addition, H_2O_2 may be spontaneously or enzymatically converted to a more reactive species that rapidly inactivates PTPs. For example, hydrogen peroxide has the potential to be converted to peroxymonophosphate or acyl peroxides capable of extremely rapid PTP inactivation (Bhattacharya, LaButti, Seiner, & Gates, 2008; LaButti, Chowdhury, Reilly, & Gates, 2007; LaButti & Gates, 2009). The conversion of H_2O_2 into peroxymonophosphate or acylperoxides would presumably require enzymatic assistance. The biological carbonate/bicarbonate buffer has been shown to potentiate the ability of H_2O_2 to inactivate PTPs (Zhou et al., 2011). This involves the spontaneous conversion of H_2O_2 to peroxymonocarbonate and seems likely to occur in the intracellular environment (Zhou et al., 2011). H_2O_2 can also react with lipids to generate lipid peroxides and, ultimately, decomposition products such as acrolein, *trans*-2-nonenal, and 4-hydroxynonenal (Conrad et al., 2010; Glascow et al., 1997; Seiner & Gates, 2007). Acrolein has been shown to inactivate purified PTP1B with an apparent second-order rate constant of (k_{inact}/K_I) of 87 M^{-1} s^{-1} (Seiner & Gates, 2007). Lipid peroxides, *trans*-2-nonenal, and 4-hydroxynonenal have been shown to inhibit PTP activity, although no rate or inhibition constants have been measured (Conrad et al., 2010; Glascow et al., 1997; Hernandez-Hernandez et al., 2005; Rinna & Forman, 2008). Along these lines, the only alkyl peroxide for which PTP inactivation rates have been measured is 2-hydroperoxytetrahydrofuran, shown to inactivate PTP1B with a rate constant of approximately 20 M^{-1} s^{-1} (Bhattacharya et al., 2008).

All of the potential mechanisms described above for the endogenous regulation of PTPs involve covalent enzyme modification. Furthermore, xenobiotics that inactivate PTPs via covalent mechanisms also have the potential to modulate signal transduction and may possess either therapeutic or toxic properties. Accurate measurement of the rate constants for chemical reactions leading to inactivation of PTPs by endogenous small molecules and xenobiotics is an important part of assessing their potential involvement in biological processes. For example, published rate constants allow the scientific community to estimate how quickly a given concentration of the agent will inactivate the protein. Covalent enzyme inactivation and reversible inhibition are fundamentally different processes, monitored and quantified by different means. The "on" rates for non-covalent binding of a reversible inhibitor to the enzyme are typically quite large (in the range

Author's personal copy

of $1 \times 10^6\ M^{-1}\ s^{-1}$), and as a result, reversible enzyme inhibition usually can be observed almost immediately upon mixing of enzyme with inhibitor (within seconds or less, Pargellis et al., 1994; an exception to this rule is slow, tight-binding inhibitors, Merkler, Brenowitz, & Schramm, 1990). In contrast, the chemical reactions involved in the covalent modification of enzymes by irreversible enzyme inactivators are usually relatively slow. Thus, covalent enzyme inactivation is often described as a "time-dependent" process, and the assays used to quantitatively determine the kinetic constants associated with covalent enzyme modification involve measuring the loss of enzyme activity over the course of minutes or hours. Here, we describe the concepts and methods underlying quantitative kinetic analysis of the covalent inactivation of PTPs by small molecules.

2. RATE EXPRESSIONS DESCRIBING COVALENT ENZYME INACTIVATION

In the case where an agent inactivates an enzyme by covalent modification without prior noncovalent association, the process may be described by the rate expression:

$$\text{Rate of inactivation} = -\frac{d[E_{act}]}{dt} = k_{obs}[I][E_{act}],$$

where $[I]$ and $[E_{act}]$ are the concentrations of inactivator and active enzyme, respectively, and k_{obs} is the observed rate constant of interest (being second order, as shown). If the concentration of inactivator is in great excess over that of enzyme (10-fold or higher), $[I]$ is effectively constant during the course of the experiment, and the rate equation may be reduced to that of a first-order process:

$$\text{Rate} = -\frac{d[E_{act}]}{dt} = k_{\psi}[E_{act}],$$

where k_{ψ} is the pseudo-first-order rate constant for the reaction and is equal to $k_{obs}*[I]$. Thus, the investigator will generally be concerned with experimentally determining k_{ψ} by first-order kinetic analysis and may determine k_{obs} by division of k_{ψ} by $[I]$.

Because loss of enzyme activity with respect to time follows first-order kinetics under pseudo-first-order conditions, such processes that "go to zero" may be described by the rate equation:

Author's personal copy

$$\frac{[E_{act}]_t}{[E_{act}]_0} = e^{-k_\psi * t},$$

where $[E_{act}]_0$ and $[E_{act}]_t$ are the concentrations of active enzyme at the start of reaction monitoring and at time t during the reaction, respectively. Note that if the reaction proceeds to some nonzero point at equilibrium, the relevant expression for generalized first-order processes is as follows:

$$\frac{[E_{act}]_t - [E_{act}]_\infty}{[E_{act}]_0 - [E_{act}]_\infty} = e^{-k_\psi * t},$$

where $[E_{act}]_\infty$ is the concentration of active enzyme at equilibrium (at $t = \infty$).

Because it is generally impractical to directly monitor the concentration of active enzyme in kinetics assays, it is common to rely on nonnatural substrates that release easy-to-measure products as an indirect readout of active enzyme concentration. A number of colorimetric and fluorometric substrates exist for the assay of PTPs (Montalibet, Skorey, & Kennedy, 2005). Thus, in the rate expressions above, we will henceforth substitute the term $[E_{act}]$ with Y, which denotes some *instrument reading*—detection of the enzyme's product—that reports indirectly upon $[E_{act}]$. Clearly, then, Y must faithfully report on the concentration of active enzyme to be of value. Therefore, we first discuss methods to ensure that the measurement of the product of enzymatic catalysis truly reflects the amount of remaining active enzyme in the PTP assay.

3. ENSURING THAT THE ENZYME ACTIVITY ASSAY ACCURATELY REFLECTS THE AMOUNT OF ACTIVE ENZYME

Before conducting enzyme inactivation assays, it is important to develop a set of assay conditions that allow accurate measurement of time-dependent losses of enzyme activity. Because *direct* mathematical substitution of Y for $[E_{act}]$ is to be made when solving the aforementioned rate equations, it is imperative that Y be linearly dependent on, and change solely as a function of, $[E_{act}]$. Note: this implicitly requires that the physical property of the molecule being measured reports linearly on its concentration – such as Abs_{410nm} does for 4-nitrophenol, under our conditions (as determined in a separate experiment). Below, we discuss methods to test whether the assay conditions give a linear relationship between enzyme

Author's personal copy

concentration and instrument response. We also discuss factors that can lead to nonlinear response and how to avoid these conditions.

3.1. Ensuring a linear response in *Y* as a function of [E_{act}]

3.1.1 Materials

PTP reaction buffer (*Buffer* "*R*"): 50 m*M* Tris, 50 m*M* Bis–Tris, 100 m*M* NaOAc, 10 m*M* DTPA, 0.5% Tween 80 (v/v), pH 7.0.

PTP activity assay buffer (*Buffer* "*A*"): 50 m*M* Bis–Tris, 100 m*M* NaCl, 10 m*M* DTPA, pH 6.0.

PTP substrate: 4-nitrophenyl phosphate (*p*NPP, disodium or di-Tris salt), made to 20 m*M* in PTP assay buffer.

Activity assay quench solution: 2 *M* NaOH in water.

Note: All buffers/aqueous solutions above are purely aqueous and should be made in highly purified water to minimize the concentration of redox-active transition metals which may oxidatively inactivate the PTP (air oxidation of thiolate in aqueous solution is a metal-dependent process; Misra, 1974).

Instruments: To maintain thermal equilibration in the reaction mixture and activity assay, a heating block or water bath will be required, and a quartz cuvette and UV–vis spectrophotometer required to measure the Abs_{410nm} of the product, 4-nitrophenolate (*p*NP).

4-Nitrophenyl phosphate provides a convenient method by which to monitor PTP activity, as PTP-mediated, catalytic hydrolysis of the substrate releases the chromophoric product 4-nitrophenol(ate), whose concentration can be measured at 410 nm and inorganic phosphate, which may also be measured if desired (Montalibet et al., 2005).

Note that, though acidification would also quench catalytic function of the PTP, it is the anion of *p*NP which absorbs strongly at 410 nm, and so a base (NaOH) quench is used to simultaneously halt the activity assay and increase signal.

3.1.2 Protocol

In a separate, preceding experiment, the concentration of the primary enzyme stock solution should be determined using standard methods (Bradford, 1976; Gilla & von Hippel, 1989; Pregel & Storer, 1997). Note that spectrophotometric determination of protein concentration requires precise knowledge of the protein sequence (Gilla & von Hippel, 1989). Additionally, these types of assays report on *total* concentration of protein in a sample; it is not necessarily the case that all protein present in the sample represents *catalytically active* enzyme. Thus, the protein concentration determined in these assays may be taken to represent the *maximum* amount of catalytically active enzyme

Author's personal copy

possible in the sample. In the analyses below, exact knowledge of the fraction of total protein that is catalytically active is not required (it *is*, however, required for the determination of k_{cat} which is defined as v_{max}/[enzyme] in Michaelis–Menten kinetics). Here, because a calibrated instrument response, *Y*, is used in place of $[E_{act}]$, we need not know its value precisely.

First, several dilutions from the concentrated primary enzyme stock are prepared and stored on ice until used. Then, to thermally-equilibrated samples of 490 μL of 20 m*M* *p*NPP in Buffer A at 30 °C are added 10 μL each of the varying-fold dilutions from the PTP stock. For the blank series, 10 μL of Buffer R alone are added to the activity assay mixture, and the sample treated identically to those containing PTP. Following addition of PTP, each sample is allowed to incubate for exactly 10 min prior to quenching of the activity assay by the addition of 500 μL of 2 *M* NaOH. The spectrophotometer is zeroed against the blank (no enzyme) assay, and the absorbance at 410 nm of each PTP-containing sample is recorded. The Abs_{410nm} readings are then plotted against the corresponding concentration of PTP in the sample (Fig. 8.1). Because each sample contains maximally active PTP, this calibration curve should represent maximal *Y* readings (Abs_{410nm}) that could be obtained if that particular concentration of enzyme were used in an inactivation experiment. Additionally, if a proper blank has been prepared, the

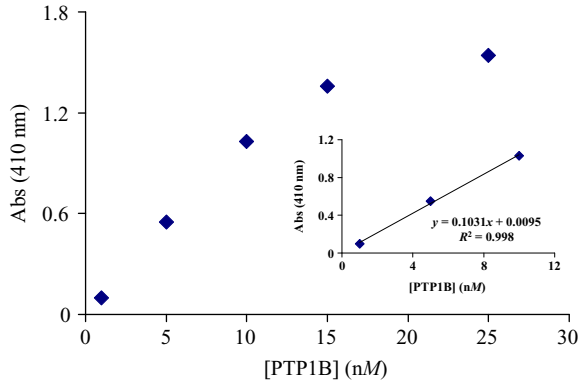

Figure 8.1 *Calibration curve for determining the range over which Y ($Abs_{410\ nm}$) is linearly dependent on concentration of PTP1B*. Several dilutions from a concentrated (20 μ*M*) stock of PTP1B were prepared and subjected to uniform activity assay conditions (20 m*M* *p*NPP, 30 °C, pH 6.0, 10 min; 500 μL total volume). Following quenching of the activity assay with 500 μL of 2 *M* NaOH, the absorbance at 410 nm was measured and plotted as a function of PTP concentration. The linear region (0–10 n*M* PTP1B) was determined to be the suitable concentration regime with which to conduct kinetics assays.

Author's personal copy

intercept of the regression line should be at the origin (x,y: $[PTP_{active}]=0$, $Y=0$). Enzyme concentrations that fall in the rising linear region of Fig. 8.1 will be suitable for enzyme inactivation experiments, as decreases in active enzyme concentration can be accurately detected in this range. On the other hand, use of enzyme concentrations in the plateau region of the plot will not be suitable for use in enzyme inactivation experiments. In this region, clearly, changes in concentration of active enzyme cannot be detected effectively. Below, we list some of the potential causes of this type of nonlinear instrument response in enzyme assays.

3.2. Some causes of nonlinearity in instrument response and associated remedies

As shown in Fig. 8.1, a plateau in Y is observed at high concentrations of PTP. In these assays, the human eye can detect that the solutions display differences in color density, yet the instrument did not detect these differences. Such lack of instrument response commonly arises when absorbance readings are above the usable range of the spectrophotometer. For most UV–vis spectrophotometers, the usable range is approximately 0–3 A.U. Note that, when absorbance readings are above the useable range of the instrument, a change in concentration of the species of interest (active PTP, reported on by [*p*NP]) does *not* necessarily afford a change in Y, thus rendering mathematical substitution of Y for $[E_{act}]$ invalid. In cases where saturation of the instrument detector occurs, the investigator may decrease the concentration of enzyme or decrease the time for which the enzyme is incubated with the substrate during the activity assay.

Most UV–vis spectrophotometers do not issue a warning to the user when readings are above the usable range of the instrument. Telltale signs of detector saturation generally involve distortions in peak shape in the absorption spectrum: frequently, detector saturation is accompanied by a flattening-out of the peak around the λ_{max} and/or a jagged form to the top of the peak. New users should beware that, if the spectrophotometer has been blanked on a strongly absorbing solution, then although subsequent readings may be *numerically* well within the "acceptable 0–3 range," the readings may, in fact, be unreliable because the total absorbance of the solution is above the working range of the instrument.

Substrate depletion is another potential cause of a plateau such as that seen in Fig. 8.1. In the case of substrate depletion, the investigator may increase the concentration of substrate, decrease the concentration of enzyme, or decrease the incubation time of the enzyme with substrate

Author's personal copy

during the activity assay. Last, we note that reaching the limit of enzyme solubility in the activity assay would also likely manifest as a plateau in Y versus $[E_{act}]$; however, this seems unlikely given that a large (50 ×) dilution of the enzyme stock solution occurs when the PTP is introduced to the activity assay mixture.

3.3. Other potential sources of error in PTP assays

Because we equate Y to $[E_{act}]$, any process that diminishes or increases the instrument reading Y will contribute to errors in the $[E_{act}]$ values used in the kinetic analysis. Here, we consider just a few potential mechanisms that can lead to errors in the instrument readings Y.

Assay conditions. Because buffer pH and temperature, depletion of substrate, and time of reaction during signal amplification all contribute to the magnitude of Y, it is of paramount importance that these factors be held constant during the activity assay, such that the sole variable responsible for changes in the reading Y is $[E_{act}]$. In practice, this is easily accomplished by using buffers of appropriate strength, maintaining thermostated reaction mixtures, ensuring sufficient substrate concentration, and rigorously controlling reaction times. Similarly, the conditions (e.g., temperature, solvent, cuvette, instrument settings, wavelength) employed for the ultimate instrumental measurement of Y in all samples must be rigorously controlled to ensure all samples are treated in an identical manner.

Interference from substrate decomposition or another absorbing species. In some assays, a species other than that of interest may contribute to the instrument reading Y. For example, in a spectrophotometric assay, an enzyme inactivator may absorb at the same wavelength as the product of the substrate used to report on enzyme activity. Two approaches are useful to correct for the undesired contribution: (1) including the appropriate concentration of the interfering species in the blank for that series negates its contribution to Y, or (2) if the former is impractical, the contribution to Y by the species may be separately determined and its contribution corrected for in the terms Y_0 and Y_∞ (thus making changes in Y_t again solely a function of $[E_{act}]$). It is also possible that decomposition of an enzyme inactivator during the assay can lead to time-dependent changes in Y that would have to be accounted for to arrive at appropriate values.

In some cases, undesired contributions to Y may arise from decomposition of the substrate employed in the assay. For example, the PTP substrate *p*NPP (Scheme 8.2) undergoes slow, nonenzymatic hydrolysis to release the pNP chromophore. Thus, in kinetics assays involving extended incubation

Author's personal copy

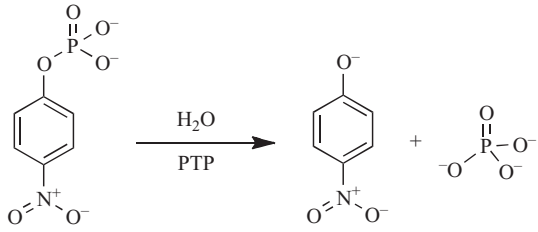

Scheme 8.2 Colorimetric PTP substrate *p*-nitrophenylphosphate (*p*NPP).

times (several hours or more), stock solutions of the enzyme substrate (*p*NPP) may begin to "yellow" and it may be necessary to rezero the spectrophotometer for each *time point* in the assay, against blanks that account for nonenzymatic hydrolysis. Doing so ensures that late reaction data do not "falsely report" an increase in concentration of active enzyme, due to the accumulation of nonenzymatically generated pNP.

Having addressed the means by which to ensure the instrument response Y faithfully reports on $[E_{act}]$, we may now turn our attention to assays that measure the rate of covalent enzyme inactivation.

4. ASSAYS FOR TIME-DEPENDENT INACTIVATION OF PTPs

4.1. General assay design considerations for a discontinuous "time-point" assay measuring time-dependent enzyme inactivation

Using the methods and concepts discussed above, it should be possible to design assay conditions that allow accurate measurement of active enzyme concentrations in an inactivation assay mixture. Thus, we are prepared to discuss the design of a discontinuous "time-point" assay that measures the kinetics of time-dependent PTP inactivation. In this type of experiment, the enzyme and the time-dependent inactivator are mixed to create an *inactivation reaction*, and at various time points, aliquots of the mixture are removed and subjected to an *activity assay* that measures the amount of active enzyme remaining at that time. Ideally, each data point taken should represent a time-frozen "snapshot" of the enzyme inactivation process. In order to accomplish this, the enzyme inactivation reaction must be stopped and remaining enzyme activity assayed. In the following section, we list several methods for stopping the enzyme inactivation reaction prior to assessment of the amount of active enzyme remaining in the aliquot:

Author's personal copy

1. *pH perturbation*: In some cases, the enzyme inactivator may be effectively quenched by acid or base. For example, protonation of anionic groups may significantly decrease the affinity of some agents for the active site of PTPs, thus decreasing their ability to carry out inactivation of the enzyme. Some reactivity is likely to remain, and time between quench and the activity assay should remain short (and consistent for all samples).
2. *Decomposition of agent*: In some cases, convenient methods for rapid decomposition of an agent may be available. For example, catalase may be used to rapidly decompose the PTP inactivator hydrogen peroxide (Halliwell & Gutteridge, 1990). Control reactions should be carried out to confirm that neither the agent employed for decomposition of the inactivator nor the products of decomposition inactivate the enzyme.
3. *Dilution of agent:* Perhaps most commonly, the inactivation reaction is abruptly halted by dilution of an aliquot of the inactivation reaction mixture directly into the activity assay mixture used to measure remaining active enzyme. Like all aforementioned methods, this approach actually serves to dramatically decrease the *rate* of reaction, rather than to completely stop it, and the decrease in rate is directly proportional to the dilution factor. Clearly, assay designs employing large dilution factors at this step will give more accurate results. In cases where the enzyme inactivator is also capable of reversible noncovalent binding to the enzyme active site (*inhibition*), residual amounts of the inactivator present following dilution into the activity assay may be sufficient to inhibit the enzyme during the assay. In these cases, at time zero, when no covalent inactivation should have occurred, the enzyme activity may be significantly below that of a control enzyme sample that contains no agent. While this may alter the appearance of the data (inactivation time courses for higher inactivator concentrations in a plot such as Fig. 8.3 will be shifted downward), analysis of the *time-dependent* loss of enzyme activity should be largely unaffected.
4. *Physical removal of the agent*: Agents may be physically removed from inactivation mixtures by various means including extraction or gel filtration. If reaction times are short, it may be somewhat challenging to execute these methods at sharply defined time points.

After the aliquot is removed from the inactivation reaction mixture and the inactivation reaction stopped, the aliquot must be subjected to an *activity assay* to measure the amount of active enzyme remaining. For accurate and reproducible results, the activity assay must be carried out in an identical manner for each time point. This typically requires a rapid quench of

Author's personal copy

enzymatic activity in the activity assay, which may be accomplished by "pH shock", addition of metal chelators (for metal-dependent enzymes), and rapid freezing.

4.2. Inactivation of PTP1B by hydrogen peroxide

Denu and Tanner (2002) provided an excellent discussion of the inactivation of PTPs by hydrogen peroxide as part of a broader review on the redox regulation of PTPs in a previous volume of this series. Our treatment of the subject is intended to provide additional technical detail. From the PTP concentration calibration curve shown in Fig. 8.1, it was determined that 8 n*M* PTP1B was suitable for use in the activity assay, under our conditions. Because this final concentration of PTP1B was achieved following a 50-fold dilution into the activity assay buffer, the requisite enzyme concentration in the inactivation reaction was calculated to be 400 n*M*. An example benchtop layout of standard laboratory equipment employed for conducting inactivation assays is presented in Fig. 8.2.

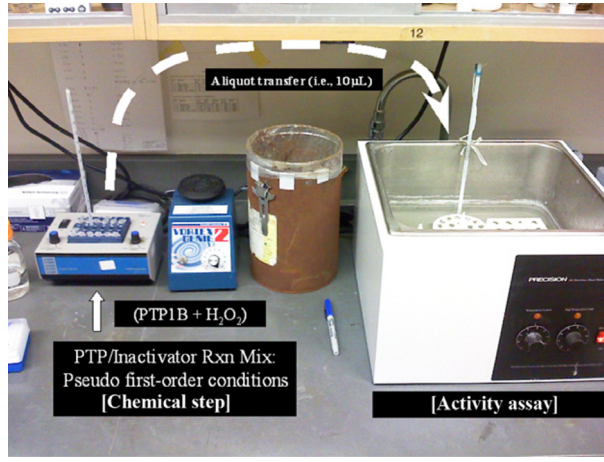

Figure 8.2 *Typical benchtop layout of equipment for enzyme kinetics assays.* A heating block (left), containing samples in which the "chemical step" (inactivation) is conducted, is maintained at the desired temperature under which the study is conducted (here, 25 °C). At predefined time intervals, aliquots are removed from the reaction mixture and diluted into ready-made activity assay mixtures (right). Here, remaining enzyme activity is assessed by permitting the enzyme to turn over substrate for a uniform period of time before quenching the reaction and measuring the concentration of product formed (e.g., $Abs_{410\ nm}$ for 4-nitrophenol).

Author's personal copy

4.2.1 Protocol

1. Free thiols were removed from a stock solution of concentrated PTP1B (20 μ*M*) by gel filtration/buffer exchange into Buffer R using a Zeba mini centrifugal desalting column (Pierce, catalog no. 89882). The stock was subsequently diluted to 0.8 μ*M* in Buffer R and stored on ice until used.
2. Prepared in Buffer R were 2×-concentrated solutions of H_2O_2: 500, 400, 300, 200, and 100 μ*M*, diluted from a 30% (wt/v) stock (Sigma). These were also stored on ice until used.
3. In 2 mL Eppendorf tubes, 490 μL (each) aliquots of 20 m*M* substrate (4-nitrophenyl phosphate, disodium hexahydrate; Sigma) in Buffer A were prepared, stored at room temperature until used (totaling 31 pre-prepared samples).
4. Just prior to starting the assay, microcentrifuge tubes containing 60 μL of 0.8 μ*M* PTP1B, and 60 μL of Buffer R containing hydrogen peroxide, were added to a heating block held at 25 °C and allowed to stand for 5 min. During that time, five activity assay samples were added to a water bath (30 °C) and allowed to thermally equilibrate.
5. The inactivation reaction was then initiated by combining 1:1 (v/v, 40 μL each) of 0.8 μ*M* PTP1B and 2×-H_2O_2 in buffer, and a timer started. At 1, 2, 4, 7, and 10 min time points during the reaction, 10 μL aliquots were removed from the inactivation mixture and diluted into the waiting 490 μL activity assay mixtures. The activity assay was allowed to proceed for 10 min before being quenched by addition of 500 μL of 2 *M* NaOH in ddH_2O (quench times of the activity assays occurred at 11, 12, 14, 17, and 20 min relative to the start of the inactivation reaction). This process was repeated for each concentration of H_2O_2 and for one control series lacking peroxide (Buffer R alone). A blank reaction sample was prepared in similar fashion: 10 μL of Buffer R alone was added to an activity assay sample and treated identically to the experimental series.
6. At the conclusion of the assay, the spectrophotometer was zeroed against the blank sample and the absorbance at 410 nm of the experimental series measured. The absorbance readings obtained in this manner were plotted as a function of time (Fig. 8.3).

5. ANALYSIS OF THE KINETIC DATA

There are many methods for analyzing enzyme inactivation data of this type. Here, we consider two broad approaches to analysis of kinetic data: (1) "traditional" linear regression analyses and (2) "modern" nonlinear curve-fitting analyses.

Author's personal copy

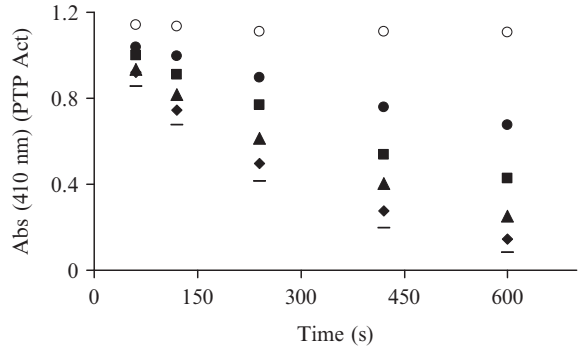

Figure 8.3 *Time-dependent inactivation of PTP1B by hydrogen peroxide under pseudo-first-order conditions.* 400 n*M* PTP1B was inactivated by various concentrations of H_2O_2 at 25 °C, pH 7.0: 250 μ*M* (dashes), 200 μ*M* (diamonds), 150 μ*M* (triangles), 100 μ*M* (squares), 50 μ*M* (closed circles), or no peroxide (open circles). Remaining enzyme activity was assayed at 1, 2, 4, 7, and 10 min intervals by dilution of 10 μL of the inactivation mixture into 490 μL of activity assay buffer. The activity assay was allowed to proceed for 10 min before quenching via addition of 500 μL of 2 *M* NaOH. The absorbance at 410 nm of each sample was then measured and plotted as a function of time, revealing exponential loss of enzyme activity versus time.

5.1. "Traditional" linear analysis

A plot of the absorbance data generated as described above yields a plot such as that seen in Fig. 8.3. Because inactivation of PTP1B by excess hydrogen peroxide affords *completely* inactive enzyme at $t = \infty$, and the blank used in the experiment accounted for any residual absorbance at 410 nm *not* from enzymatic hydrolysis, the Y_∞ value can be taken as zero. The initial measurement, Y_0, need not *actually* be that corresponding to the "real" $t = 0$ (measurement of which is effectively impossible). Rather, Y_0 represents the first *monitoring* of the reaction, relative to which all Y_t values are spaced with respect to time. For our purposes here, the first collected data point in the control series (no H_2O_2) series has been defined as Y_0 for all experimental series.

5.1.1 Extraction of pseudo-first-order rate constants by linear analysis

Having defined all parameters (Y_0, Y_∞, and Y_t), a plot of the natural logarithm of percent remaining activity versus time may be generated; namely: ln $((Y_t/Y_0) * 100)$ versus time. It is worth noting that plotting the natural logarithm of "simple" (not percent) remaining activity versus time affords the same numerical results, but a perhaps less aesthetically pleasing graphical form, as the natural logarithm of numbers less than 1 are negative.

Author's personal copy

Having generated the replot (Fig. 8.4), the resulting transformation should be carefully inspected for strict linearity. As will be described later, nonlinear behavior in this plot is indicative of either non-first-order kinetics or use of an inappropriate Y_∞ value (Fig. 8.5).

Once it has been determined that the data adhere to linearity in the "ln plot," linear regression analysis may be performed for each series (i.e., for each concentration of inactivator). Because the kinetics of a pseudo-first-order process is described by

$$\ln\frac{Y_t}{Y_o} = -k_\psi * t,$$

where k_ψ is the pseudo-first-order rate constant, a plot of $\ln(Y_t/Y_0)$ versus time affords lines with slopes $-k_\psi$. Thus, the negative of the slope of each line equals the pseudo-first-order rate constant for the corresponding concentration of inactivator (with units of reciprocal time corresponding to that used on the *X*-axis).

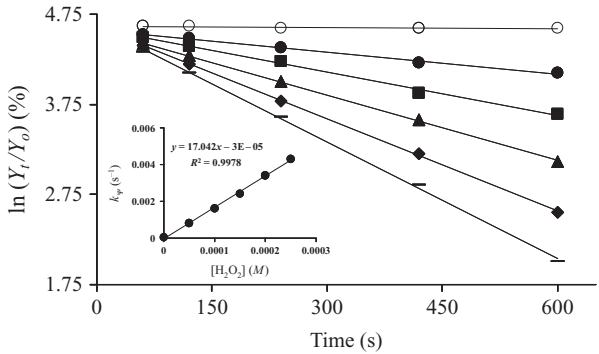

Figure 8.4 *Analysis of inactivation kinetic data via linear methods.* The $Abs_{410\ nm}$ readings from the inactivation assay were replotted as the natural logarithms of percent remaining activity (relative to the control) versus time. The replot afforded straight lines, in agreement with a (pseudo)-first-order process. The slope of the linear regression trendline from each series is equal to the negative of the pseudo-first-order rate constant, for inactivation of PTP1B by the corresponding concentration of H_2O_2. A replot of the pseudo-first-order rate constants versus concentration of inactivator affords a straight line which passes through the origin, in agreement with a simple bimolecular process in the rate-determining step (inset). The slope of this line is the apparent bimolecular rate constant for inactivation of PTP1B by H_2O_2 under our conditions, with units of $M^{-1}\ s^{-1}$.

Author's personal copy

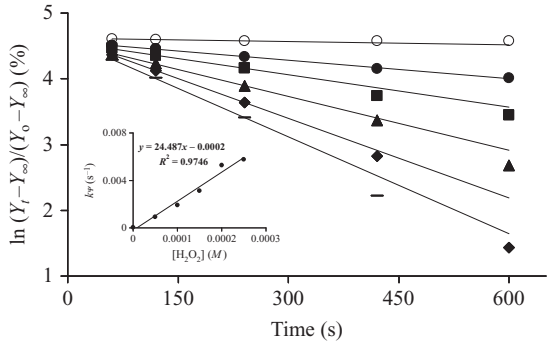

Figure 8.5 *Replot of natural logarithm of percent remaining activity with inappropriate choice of* Y_∞. Kinetic data from inactivation of PTP1B by H_2O_2 were analyzed by linear methods: here, with intentional choice of an inappropriate Y_∞ value (here, 0.1 A.U. instead of 0 A.U. at 410 nm). Appreciable curvature is noted in the data, especially as Y_t approaches Y_∞. This curvature is indicative of a poor determination of Y_∞. The calculated bimolecular rate constant of interest is "skewed" as a consequence of this selection of Y_∞ (inset). To better highlight curvature in the data, the regression trendlines shown only consider the early (first three) data points from each series.

Though, in principle, one could conduct a single assay under pseudo-first-order conditions and extract an apparent bimolecular rate constant by dividing k_ψ by the concentration of inactivator, this represents an incomplete and potentially erroneous approach to describing the kinetics of a process. The more rigorous and informative approach is to examine the dependence of the pseudo-first-order rate constants on concentration of inactivator. As shown in Fig. 8.4 (inset), the pseudo-first-order rate constant for inactivation of PTP1B by H_2O_2 is linearly dependent upon concentration of H_2O_2. Such linear dependence is not universal for all PTP inactivators, and the interpretation of these data is described at the end of this work.

5.1.2 Linear analysis methods: Strengths and weaknesses

Although contemporary computational abilities long ago dispensed with the *necessity* for linear (graphical) analyses of data, it is still a highly useful and straightforward approach. Linear analysis benefits from being "user-friendly," precise, and accurate when used in conjunction with good experimental data and requires little or no specialized software or training. Analysis of linearized data is typically very straightforward, and large deviations from linearity in a data set generally are easy to spot.

The chief drawbacks of linear methods for analysis involve treatment of "late data" and intercept evaluation. Regarding treatment of late data, as Y_t

Author's personal copy

approaches Y_∞, two issues arise: (1) because the dynamic changes in Y_t can become small with respect to the error inherent in making the measurement, the data sometimes become erratic and essentially useless in the ln replot; and (2) as the dynamic character of the measurement approaches zero (as Y_t approaches Y_∞, a constant), the data may again be unusable in linear analysis, as a consequence of there being no measurable change in activity versus time. If there is no measurable change in activity versus time, then there can be no change in ln (%) activity versus time, and the slope of the regression line in the ln replot will bend to zero. Additionally, in late data, small errors in the determination of Y_∞ become more pronounced, often resulting in an obvious curvature of the data in the ln replot, which *should be* linear (Fig. 8.5 depicts such curvature). As discussed in the next section, curve-fitting methods adapt well to, but are certainly not immune to these issues.

The second general weakness associated with linear regression analyses involves determination of values that are computed as intercepts, such as is done with the Kitz–Wilson plot (Fig. 8.6; Kitz & Wilson, 1962; Silverman, 2000). Values determined from intercepts along the *X*- or *Y*-axis may be subject to exaggerated error when the experimental data fall "far"

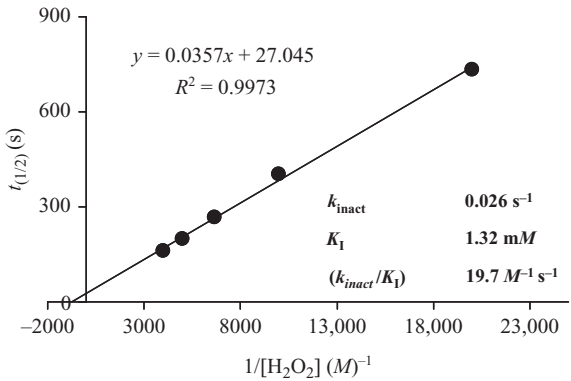

Figure 8.6 *Kitz–Wilson replot of kinetic data for inactivation of PTP1B by H_2O_2.* The Kitz–Wilson replot is commonly used in analysis of kinetic data of inactivators which have noncovalent affinities for their protein targets (e.g., affinity labeling agents). For inactivators which have no appreciable affinity, the linear regression trendline in the Kitz–Wilson plot should intercept at the origin. Here, small experimental errors afford a nonorigin intercept, as hydrogen peroxide is not known to possess any particular affinity for the active site of PTP1B. Thus, the physical interpretation of the intercept is ambiguous in this case.

Author's personal copy

from the axis at which the intercept occurs in the replot. Under these circumstances, small errors in the data may dramatically alter the values of the intercepts. For example, in the Kitz–Wilson plot, the *y*-intercept is equal to $\ln(2)/k_{\text{inact}}$, and the *x*-intercept to $(-)1/K_{\text{I}}$. Because the *X*-axis has units of reciprocal concentration, but the *x*-intercept is *negative*, the *x*-intercept *must* be calculated by projections made based on experimental data. It stands to reason, then, that the only way good projections can be made is by having collected excellent experimental data.

5.2. Nonlinear curve-fitting regression analysis

For this consideration of curve-fitting analysis, we will employ the same kinetic data used above in the linear regression analysis. The parameters defined above will be used in identical fashion here (those of Y_t, Y_0, and Y_∞). Conceptually, the approach is very similar: starting from the rearranged integrated rate law for a first-order process, we see that there is an exponential dependence of Y_t on both the (pseudo)-first-order rate constant and time:

$$Y_t = Y_o e^{-k_\psi * t}$$

Because Y_0 and Y_t are measured quantities, and the time intervals at which the process was monitored are known, the only parameter to be optimized to make the mathematical model fit the experimental data is the rate constant of interest, k_ψ.

The parameter optimization process (data fitting) may be accomplished with a variety of software suites, including Prism and Microsoft Excel. Independent of software package used, most commonly the essence of the fitting process involves computing the arithmetic differences between model and experimental data sets for each data point, squaring these differences, and finally minimizing the sum of these squared differences by modulating the parameter to be optimized (here, k_ψ). Finally, the optimized data set (from which k_ψ is determined) should be graphically compared against the empirical data set for visual inspection of agreement between the two (Fig. 8.7). Additionally, examining a plot of the residuals is a rigorous method by which to identify any systematic bias in the fitted data set. An excellent discussion of several ways by which this may be done is freely available on the NIST Web site (Anonymous). The optimized parameters that afford the best fit of the model to the experimental data set are taken to be the appropriate values of interest (here, k_ψ). Figure 8.7 shows an example

Author's personal copy

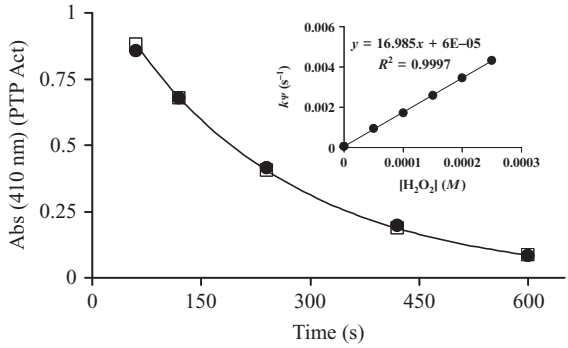

Figure 8.7 *Analysis of inactivation kinetic data via nonlinear regression analysis.* The untransformed experimental data ($Abs_{410\ nm}$ vs. time) were used to fit model first-order kinetic data, with k_ψ as the only adjustable parameter (Y_0 and Y_∞ were defined in identical fashion to that of the linear analysis method). No constraints were placed on k_ψ during the optimization process. The optimized, fitted model was graphically examined for goodness of fit. Shown are the experimental data for the inactivation of PTP1B by 250 μM H_2O_2 (closed circles) and the fitted model data (open squares and trendline) from which k_ψ was determined. This process was repeated for each concentration of H_2O_2, and the optimized k_ψ values were plotted as a function of corresponding concentration of H_2O_2. This afforded a straight line in the replot which passes through the origin, indicative of a simple bimolecular reaction. The calculated bimolecular rate constant is in excellent agreement with that determined by linear analysis methods ($17\ M^{-1}\ s^{-1}$).

of a model set fitted to the experimental data, where the only parameter optimized was k_ψ. This process was repeated for each concentration of inactivator, and the resulting series of pseudo-first-order rate constants were plotted against corresponding concentrations of H_2O_2. A linear dependence of k_ψ on $[H_2O_2]$ was again observed (Fig. 8.7, inset), and the apparent bimolecular rate constant was found to be in excellent agreement with that computed by linear graphical analysis methods ($17\ M^{-1}\ s^{-1}$ in both cases).

5.2.1 Curve-fitting analysis: Strengths and weaknesses

In order to speak meaningfully about the pitfalls of nonlinear regression analysis, we must first consider its strengths. Nonlinear regression analysis is an exceedingly powerful tool; it is very flexible, being well suited for the treatment of an entire data set, from "start to finish." Furthermore, if an accurate determination of Y_∞ was not experimentally made, the methods of nonlinear regression analysis allow Y_∞ itself to be an adjustable parameter, in addition to k_ψ. This facet is extremely useful for sluggish reactions, or for reactions which proceed to different Y_∞ values as a function of concentration of inactivating species. In these cases, collection of large amounts of

Author's personal copy

"late-phase" reaction data actually facilitates accurate optimization of adjustable parameters, as the data are used to better determine appropriate values for the parameters being optimized (especially for Y_∞). Additionally, the investigator may define a numerical range into which the parameters must fall during/at the conclusion of the optimization process, such that values determined from empirically–collected data are used to bound upper and lower limits of any adjustable parameter. Taken together, nonlinear regression represents an exceedingly useful tool for kinetic analysis, allowing the investigator to decide which parameters to leave fixed or to make adjustable, and to define the window into which adjustable parameters must ultimately fall.

The reader may be struck by the last statement, understanding immediately some potentially crippling pitfalls of nonlinear regression analysis. If the investigator selects an inappropriate window into which any given parameter may fall, the kinetic analysis becomes invalid (the magnitude of invalidity being directly proportional to "how far off the mark" the prescribed window was set). It is no surprise, then, that parameters which are to be fit must be "bracketed" (bounded) with great care. Despite the obvious potential for mistakes in this regard, this aspect of data fitting is typically not of the greatest concern, as appropriate windows in which to bound optimized parameters are generally clear from the empirical data (e.g., following a reaction through three half-lives limits the maximum error in optimization of Y_∞ to roughly 10%).

Perhaps the greatest drawback to nonlinear regression analysis is the challenge of discerning when a good-*looking* fit of the model to the experimental data *does not* provide realistic kinetic values. This so-called chi-by-eye approach, referring to visual evaluation of goodness of fit by graphical methods, can be highly misleading. Furthermore, deviations from the expected graphical form may be more difficult to spot in curvilinear data than in linear data during visual analysis. It is the author's experience that the greatest potential for erroneous analysis of kinetic data by nonlinear regression methods arises when fitting "early reaction data" with a poorly defined Y_∞ value. It is a logical extension to suggest that such erroneous analysis would also apply when analyzing "late-phase" reaction data with a poorly defined Y_0 (though, for reasons stated earlier, this is probably less likely a concern). The fundamental rationale for these observations may be that, in many reactions, "early" and "late" data appear linear in form, and so do not adequately reflect the exponential nature of the data expected for the full time course (to which the model is fit). Unfortunately, when

Author's personal copy

fitting data sets containing only "early data," the optimized model may look deceptively well fit to the experimental data, though the optimized parameters have very poor agreement with those of physical reality (the "true values"). For these reasons, it is crucial that the investigator adequately defines the window into which adjustable parameters are to fall and very critically evaluates the optimized parameters at the end of the fitting process, with respect to their empirical viability (i.e., do the values "make sense" with respect to what the investigator knows about the assay?).

6. OBTAINING AN INACTIVATION RATE CONSTANT FROM THE DATA

Having collected and analyzed the kinetic data, and extracted pseudo-first-order rate constants by linear or curve-fitting methods, the investigator may now begin to characterize the kinetic properties of the process of interest. Here, we briefly cover two kinetic profiles observed for PTP inactivators and refer the reader elsewhere for a more complete discussion of analysis of pseudo-first-order kinetics (Espenson, 1995).

As shown in Figs. 8.4 and 8.7 (insets), a plot of the pseudo-first-order rate constants (in s^{-1}) versus molar concentration of the inactivator H_2O_2 affords a straight line that passes through the origin. The graphical form of this plot (linear, intercepting the origin) suggests a simple bimolecular process in the rate-determining step, that is first order in inactivator. The slope of the line is the observed bimolecular rate constant (in $M^{-1}\,s^{-1}$) for inactivation of PTP1B by H_2O_2, under these conditions. Indeed, this is perhaps the simplest kinetic profile for a bimolecular reaction.

Another common graphical form the investigator may encounter is the "saturation profile" in the plot of k_ψ versus concentration of inactivator (Fig. 8.8). In similar fashion to the principles underlying traditional Michaelis–Menten kinetics with *substrate*s, this behavior is a result of reversible, noncovalent association of the inactivator with the enzyme prior to the chemical inactivation step (Scheme 8.3). Here, the enzyme first reversibly binds the inactivator, rapidly forming the $E{\cdot}I$ complex by the second-order rate constant k_{on}. The $E{\cdot}I$ complex may then collapse back to free enzyme and inhibitor by rate constant k_{off}, or covalent modification/inactivation of the enzyme may occur by rate constant k_{inact} (both rate constants being first order). Because the chemical step, represented by $k_{inact}[E{\cdot}I]$, is usually rate limiting, increasing the concentration of the $E{\cdot}I$ complex increases the observed rate of inactivation. At low concentrations of inhibitor, increasing

Author's personal copy

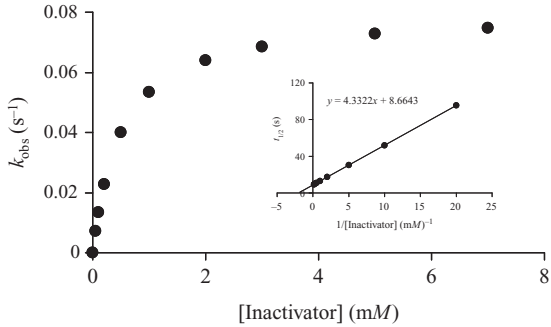

Figure 8.8 *Mock data: "saturation profile" for an inactivator which has affinity for its enzyme target.* For inactivating species which possess affinity for their targets (such as affinity labeling agents), saturation kinetics may be observed in the rate of inactivation at high concentrations of inactivator. The kinetic parameters k_{inact} and K_I may be extracted by linear methods (e.g., Kitz–Wilson replot, inset), or by curve-fitting methods. Here, the mock data were generated using $k_{inact} = 0.08\ s^{-1}$ and $K_I = 500\ \mu M$.

$$E + I \underset{k_{off}}{\overset{k_{on}}{\rightleftharpoons}} E{\cdot}I \xrightarrow{k_{inact}} E{-}I$$

Scheme 8.3 Inactivation of PTPs by affinity labeling agents.

the concentration of the inhibitor drives formation of the $E{\cdot}I$ complex, resulting in an increase in observed rate of inactivation. However, when essentially all enzyme is occupied in the $E{\cdot}I$ complex under saturating concentrations of inactivator, further increases in concentration of inactivator do *not* result in increased rates of inactivation. Consequently, the observed rate of inactivation becomes *independent* of inactivator concentration under saturating conditions, resulting in a plateau in the plot of k_ψ versus [inactivator]. Note that reaching the limit of solubility of the inactivator may also result in such a plateau, and the investigator should confirm that this is not the underlying cause of the plateau in observed rates of inactivation at high inactivator concentrations.

Analysis of this type of kinetic data may be accomplished by the Kitz–Wilson plot (Fig. 8.8, inset; Kitz & Wilson, 1962; Silverman, 2000). The Kitz–Wilson plot is a convenient tool with which the investigator may determine both K_I and k_{inact}. However, for reasons described earlier, the investigator should take care in data collection for and evaluation of intercept-based values. Alternatively, these data may be evaluated using curve-fitting methods. For example, Zhang's group identified inactivators

Author's personal copy

of PTP1B which exhibit saturation behavior and determined the parameters K_I and k_{inact} by fitting to, essentially, the Michaelis–Menten equation, with K_I in place of K_m and k_{inact} in place of V_{max} (Liu et al., 2008).

7. SUMMARY

Here, we have described some fundamental considerations to be made when monitoring the activity of enzyme systems, the general conceptual bases underlying assay design when measuring the rates of covalent enzyme modification, and several methods by which the kinetic data may be analyzed. We have also reported a detailed method by which the rate of inactivation of PTP1B by hydrogen peroxide may be determined; this method may be extended to other inactivators, and to other PTPs. Finally, we have addressed the merits and drawbacks to numerous methods of data analysis, with an eye toward "choosing the right tool for the job."

REFERENCES

Anonymous. National Institutes of Standards and Technology website. http://wwwitlnistgov/div898/handbook/indexhtm.

Barr, A. J., Ugochukwu, E., Lee, W. H., King, O. N., Filippakopoulos, P., Alfano, I., et al. (2009). Large-scale structural analysis of the classical human protein tyrosine phosphatome. *Cell*, *136*, 352–363.

Bhattacharya, S., LaButti, J. N., Seiner, D. R., & Gates, K. S. (2008). Oxidative inactivation of PTP1B by organic peroxides. *Bioorganic & Medicinal Chemistry Letters*, *18*, 5856–5859.

Bradford, M. (1976). Rapid and sensitive method for the quantification of microgram quantities of protein utilizing the principle of protein-dye binding. *Analytical Biochemistry*, *72*, 248–254.

Chen, K., Kirber, M. T., Yang, Y., & Keaney, J. F. J. (2008). Regulation of ROS signal transduction by NADPH oxidase 4 localization. *The Journal of Cell Biology*, *181*, 1129–1139.

Conrad, M., Sandin, A., Förster, H., Seiler, A., Frijhoff, J., Dagnell, M., et al. (2010). 12/15-Lipoxygenase-derived lipid peroxides control receptor protein kinase signaling through oxidation of protein tyrosine phosphatases. *Proceedings of the National Academy of Sciences of the United States of America*, *107*, 15774–15779.

den Hertog, J., Groen, A., & van der Wijk, T. (2005). Redox regulation of protein-tyrosine phosphatases. *Archives of Biochemistry and Biophysics*, *434*, 11–15.

Denu, J. M., & Tanner, K. G. (1998). Specific and reversible inactivation of protein tyrosine phosphatases by hydrogen peroxide: Evidence for a sulfenic acid intermediate and implications for redox regulation. *Biochemistry*, *37*, 5633–5642.

Denu, J. M., & Tanner, K. G. (2002). Redox regulation of protein tyrosine phosphatases by hydrogen peroxide: Detecting sulfenic acid intermediates and examining reversible inactivation. *Methods in Enzymology*, *348*, 297–305.

Dickinson, B. C., & Chang, C. J. (2011). Chemistry and biology of reactive oxygen species in signaling and stress responses. *Nature Chemical Biology*, *7*, 504–511.

Espenson, J. H. (1995). *Chemical kinetics and reaction mechanisms* (2nd ed.). New York: McGraw-Hill, Inc.

Author's personal copy

Gilla, S. C., & von Hippel, P. H. (1989). Calculation of protein extinction coefficients from amino acid sequence data. *Analytical Biochemistry*, *182*, 319–326.

Glascow, W. C., Hui, R., Everhart, A. L., Jayawickreme, S. P., Angerman-Stewart, J., Han, B.-B., et al. (1997). The linoleic acid metabolite, (13S)-hydroperoxiyocta-decadienoic acid, augments the epidermal growth factor receptor signaling pathway by attenuation of receptor dephosphorylation. *The Journal of Biological Chemistry*, *272*, 19269–19276.

Halliwell, B., & Gutteridge, J. M. C. (1990). Role of free radicals and catalytic metal ions in human disease: An overview. *Methods in Enzymology*, *186*, 1–85.

Hecht, D., & Zick, Y. (1992). Selective inhibition of protein tyrosine phosphatase activities by H_2O_2 and vanadate in vitro. *Biochemical and Biophysical Research Communications*, *188*, 773–779.

Heffetz, D., Bushkin, I., Dror, R., & Zick, Y. (1990). The insulinomimetic agents H_2O_2 and vanadate stimulate protein tyrosine phosphorylation in cells. *The Journal of Biological Chemistry*, *265*, 2896–2902.

Hernandez-Hernandez, A., Garabatos, M. N., Rodriguez, M. C., Vidal, M. L., Lopez-Revuelta, A., Sanchez-Gallego, J. I., et al. (2005). Structural characteristics of a lipid peroxidation product, trans-2-nonenal, that favour inhibition of membrane-associated phosphotyrosine phosphatase activity. *Biochimica et Biophysica Acta*, *1726*, 317–325.

Hunter, T. (2000). Signaling—2000 and beyond. *Cell*, *100*, 113–127.

Kitz, R., & Wilson, I. B. (1962). Esters of methanesulfonic acid as irreversible inhibitors of acetylcholinesterase. *The Journal of Biological Chemistry*, *237*, 3245–3249.

LaButti, J. N., Chowdhury, G., Reilly, T. J., & Gates, K. S. (2007). Redox regulation of protein tyrosine phosphatase 1B by peroxymonophosphate. *Journal of the American Chemical Society*, *129*, 5320–5321.

LaButti, J. N., & Gates, K. S. (2009). Biologically relevant properties of peroxymonophosphate (=O3POOH). *Bioorganic & Medicinal Chemistry Letters*, *19*, 218–221.

Lambeth, J. D. (2004). NOX enzymes and the biology of reactive oxygen. *Nature Reviews. Immunology*, *4*, 181–189.

Lambeth, J. D., Kawahara, T., & Diebold, B. (2007). Regulation of Nox and Duox enzymatic activity and expression. *Free Radical Biology & Medicine*, *43*, 319–331.

Lee, S. R., Kwon, K. S., Kim, S. R., & Rhee, S. G. (1998). Reversible inactivation of protein-tyrosine phosphatase 1B in A431 cells stimulated with epidermal growth factor. *The Journal of Biological Chemistry*, *273*, 15366–15372.

Lemmon, M. A., & Schlessinger, J. (2010). Cell signaling by receptor tyrosine kinases. *Cell*, *141*, 1117–1134.

Liu, S., Yang, H., He, Y., Jiang, Z.-H. , Kumar, S., Wu, L., et al. (2008). Aryl vinyl sulfonates and sulfones as active site-directed and mechanism-based probes for protein tyrosine phosphatases. *Journal of the American Chemical Society*, *130*, 8251–8260.

Mahedev, K., Zilbering, A., Zhu, L., & Goldstein, B. J. (2001). Insulin-stimulated hydrogen peroxide reversibly inhibits protein-tyrosine phosphatase 1B in vivo and enhances the early insulin action cascade. *The Journal of Biological Chemistry*, *276*, 21938–21942.

Meng, T.-C. , Buckley, D. A., Galic, S., Tiganis, T., & Tonks, N. K. (2004). Regulation of insulin signaling through reversible oxidation of the protein tyrosine phosphatases TC45 and PTP1B. *The Journal of Biological Chemistry*, *279*, 37716–37725.

Merkler, D. J., Brenowitz, M., & Schramm, V. L. (1990). The rate constant describing slow-onset inhibition of yeast AMP deaminase by coformycin analogues is independent of inhibitor structure. *Biochemistry*, *29*, 8358–8364.

Misra, H. P. (1974). Generation of superoxide free radical during the autooxidation of thiols. *The Journal of Biological Chemistry*, *249*, 2151–2155.

Montalibet, J., Skorey, K. I., & Kennedy, B. P. (2005). Protein tyrosine phosphatase: Enzymatic assays. *Methods*, *35*, 2–8.

Author's personal copy

Östman, A., Frijhoff, J., Sandin, A., & Böhmer, F.-D. (2011). Regulation of protein tyrosine phosphatases by reversible oxidation. *The Biochemical Journal*, *150*, 345–356.

Pargellis, C. A., Morelock, M. M., Graham, E. T., Kinkade, P., Pav, S., Lubbe, K., et al. (1994). Determination of kinetic rate constants for the binding of inhibitors to HIV-1 protease and for the association and dissociation of active homodimer. *Biochemistry*, *33*, 12527–12534.

Parsons, Z. D., & Gates, K. S. (2013). Thiol-dependent recovery of catalytic activity from oxidized protein tyrosine phosphatases. *Biochemistry*, Manuscript under revision.

Pregel, M. J., & Storer, A. C. (1997). Active site titration of tyrosine phosphatases SHP-1 and PTP1B using aromatic disulfides. *The Journal of Biological Chemistry*, *272*, 23552–23558.

Rhee, S. G. (2006). H_2O_2, a necessary evil for cell signaling. *Science*, *312*, 1882–1883.

Rinna, A., & Forman, H. J. (2008). SHP-1 inhibition by 4-hydroxynonenal activates Jun N-terminal kinase and glutamate cysteine ligase. *American Journal of Respiratory Cell and Molecular Biology*, *39*, 97–104.

Seiner, D. R., & Gates, K. S. (2007). Kinetics and mechanism of protein tyrosine phosphatase 1B inactivation by acrolein. *Chemical Research in Toxicology*, *20*, 1315–1320.

Silverman, R. B. (2000). *The organic chemistry of enzyme-catalyzed reactions*. San Diego: Academic Press.

Sivaramakrishnan, S., Cummings, A. H., & Gates, K. S. (2010). Protection of a single-cysteine redox switch from oxidative destruction: On the functional role of sulfenyl amide formation in the redox-regulated enzyme PTP1B. *Bioorganic & Medicinal Chemistry Letters*, *20*, 444–447.

Sivaramakrishnan, S., Keerthi, K., & Gates, K. S. (2005). A chemical model for the redox regulation of protein tyrosine phosphatase 1B (PTP1B). *Journal of the American Chemical Society*, *127*, 10830–10831.

Stone, J. R. (2006). Hydrogen peroxide: A signaling messenger. *Antioxidants & Redox Signaling*, *8*, 243–270.

Tanner, J. J., Parson, Z. D., Cummings, A. H., Zhou, H., & Gates, K. S. (2011). Redox regulation of protein tyrosine phosphatases: Structural and chemical aspects. *Antioxidants & Redox Signaling*, *15*, 77–97.

Tarrant, M. K., & Cole, P. A. (2009). The chemical biology of protein phosphorylation. *Annual Review of Biochemistry*, *78*, 797–825.

Tonks, N. K. (2006). Protein tyrosine phosphatases: From genes, to function, to disease. *Nature Reviews. Molecular Cell Biology*, *7*, 833–846.

Truong, T. H., & Carroll, K. S. (2012). Redox-regulation of EGFR signaling through cysteine oxidation. *Biochemistry*, *51*, 9954–9965.

Ushio-Fukai, M. (2006). Localizing NADPH oxidase-derived ROS. *Science STKE*, *349*, 1–6.

Winterbourn, C. C. (2008). Reconciling the chemistry and biology of reactive oxygen species. *Nature Chemical Biology*, *4*, 278–286.

Woo, H. A., Yim, S. H., Shin, D. H., Kang, D., Yu, D.-Y. , & Rhee, S. G. (2010). Inactivation of peroxiredoxin I by phosphorylation allows localized hydrogen peroxide accumulation for cell signaling. *Cell*, *140*, 517–528.

Zhou, H., Singh, H., Parsons, Z. D., Lewis, S. M., Bhattacharya, S., Seiner, D. R., et al. (2011). The biological buffer, bicarbonate/CO_2, potentiates H_2O_2-mediated inactivation of protein tyrosine phosphatases. *Journal of the American Chemical Society*, *132*, 15803–15805.